IR Observations of a Flaring Maser Source
-
Revealing the Unsteady Growth of Massive Stars

B. Stecklum, V. Wolf, J. Eislöffel (TLS), A. Caratti o Garatti (DIAS),
Ch. Fischer (DSI), H. Linz (MPIA), T.J. Harries (UExeter) & M2O collaboration

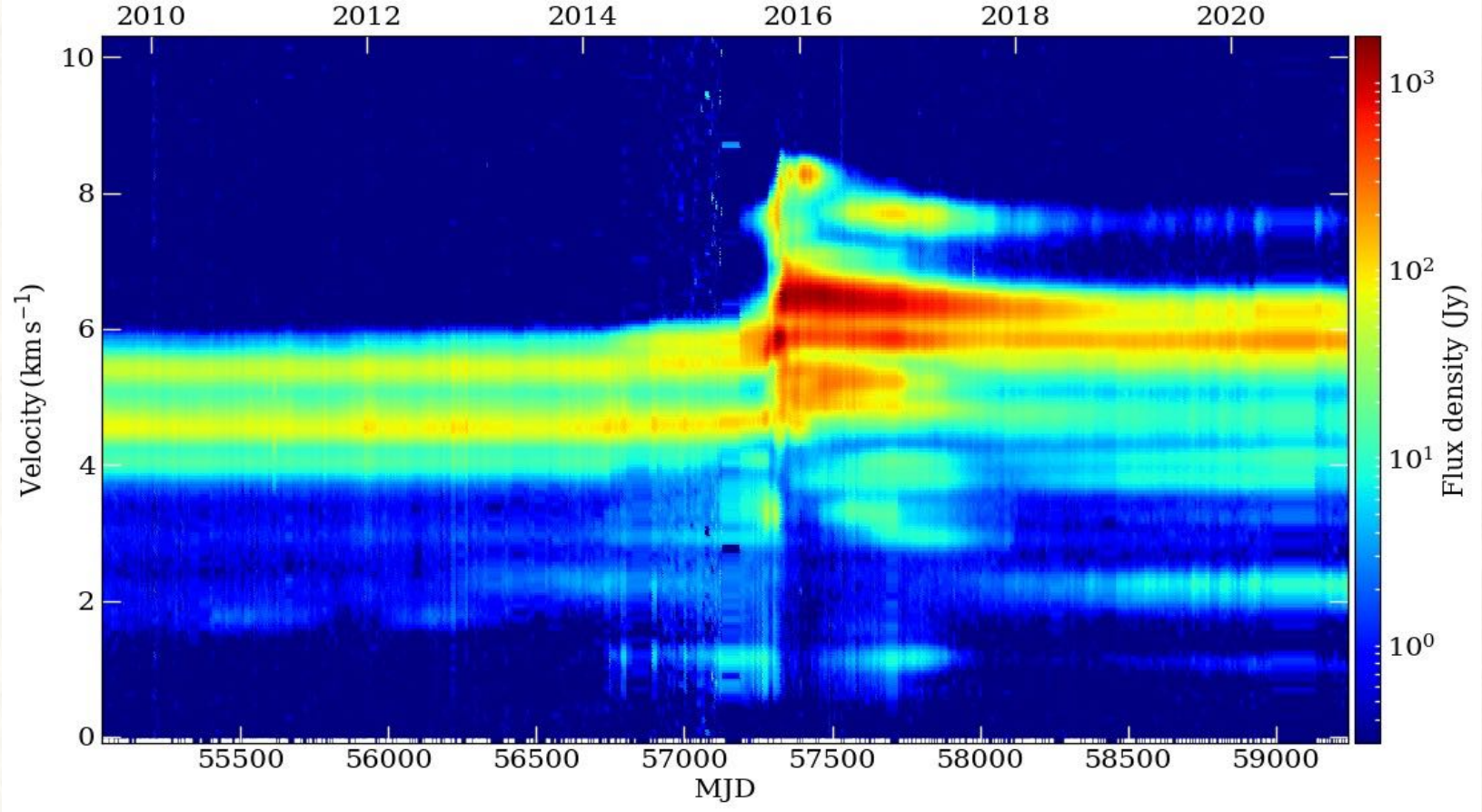

Dynamic spectrum of the 6.7GHz methanol maser of S255IR-NIRS3 (© M. Durjasz)

Outline of the Talk

- **Episodic accretion of low-mass YSOs – From T Tauri to proto-stars**
- **Accretion bursts from MYSOs – An extraordinary coincidence**
- **Methanol maser alerts – M2O's first catch: G358**
- **Modeling of the thermal afterglow**
- **How to "weigh" the accreted mass using SOFIA**
- **Heat-wave propagation and maser relocation**
- **Implications of accretion bursts**
- **Prospects and summary**

Episodic Accretion of Low-Mass YSOs
–
From T Tauri to Proto-Stars

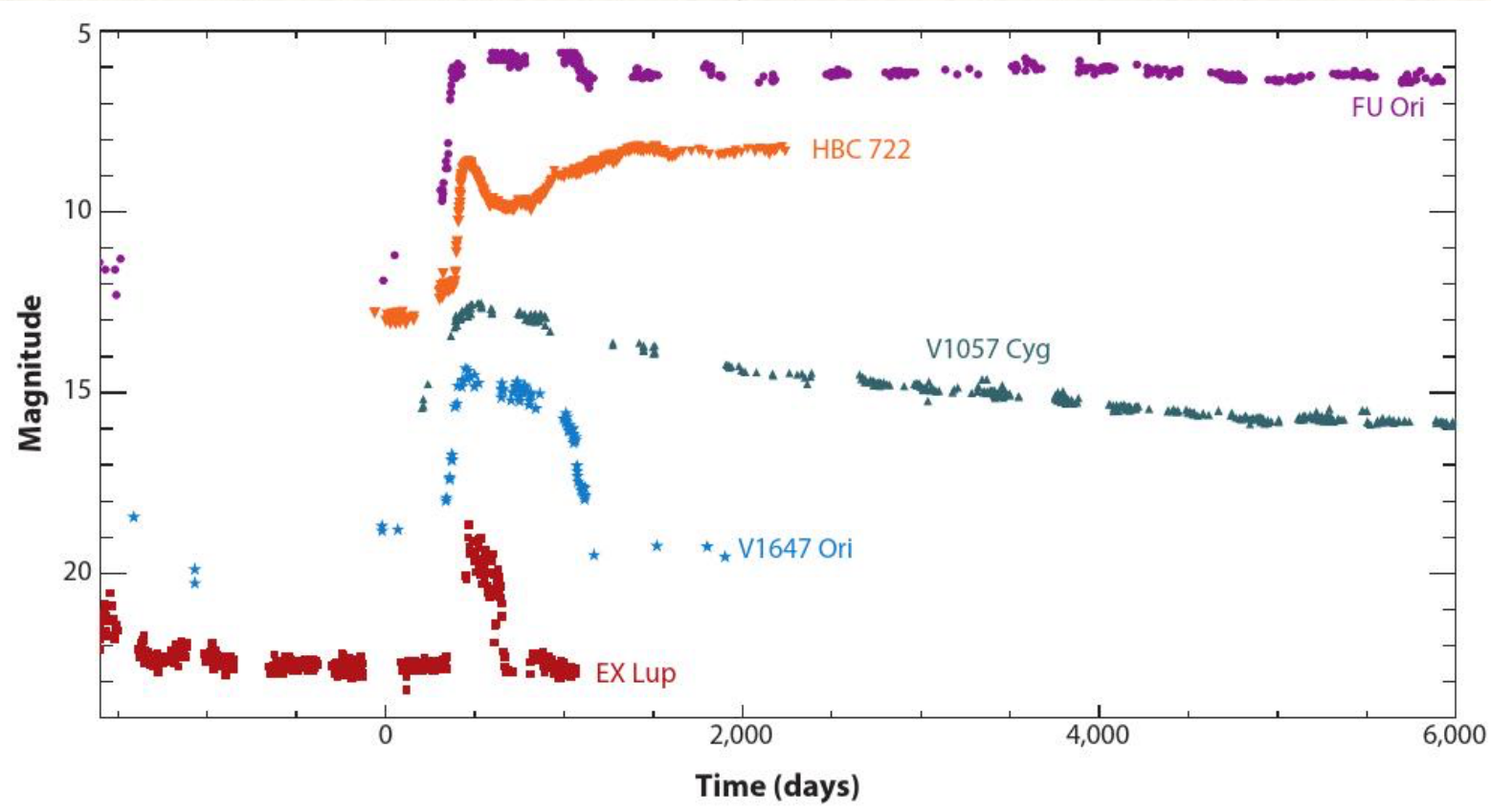

Optical light curves of T-Tauri star accretion bursts (Kospal+ 2011).
FU Ori and EX Lup are the templates for FUors and EXors.

$$L = L_* + \frac{G M_*}{R_*} \dot{M}_{acc}$$

Luminosity due to contraction and accretion

Episodic Accretion of Low-Mass YSOs
–
From T Tauri to Proto-Stars

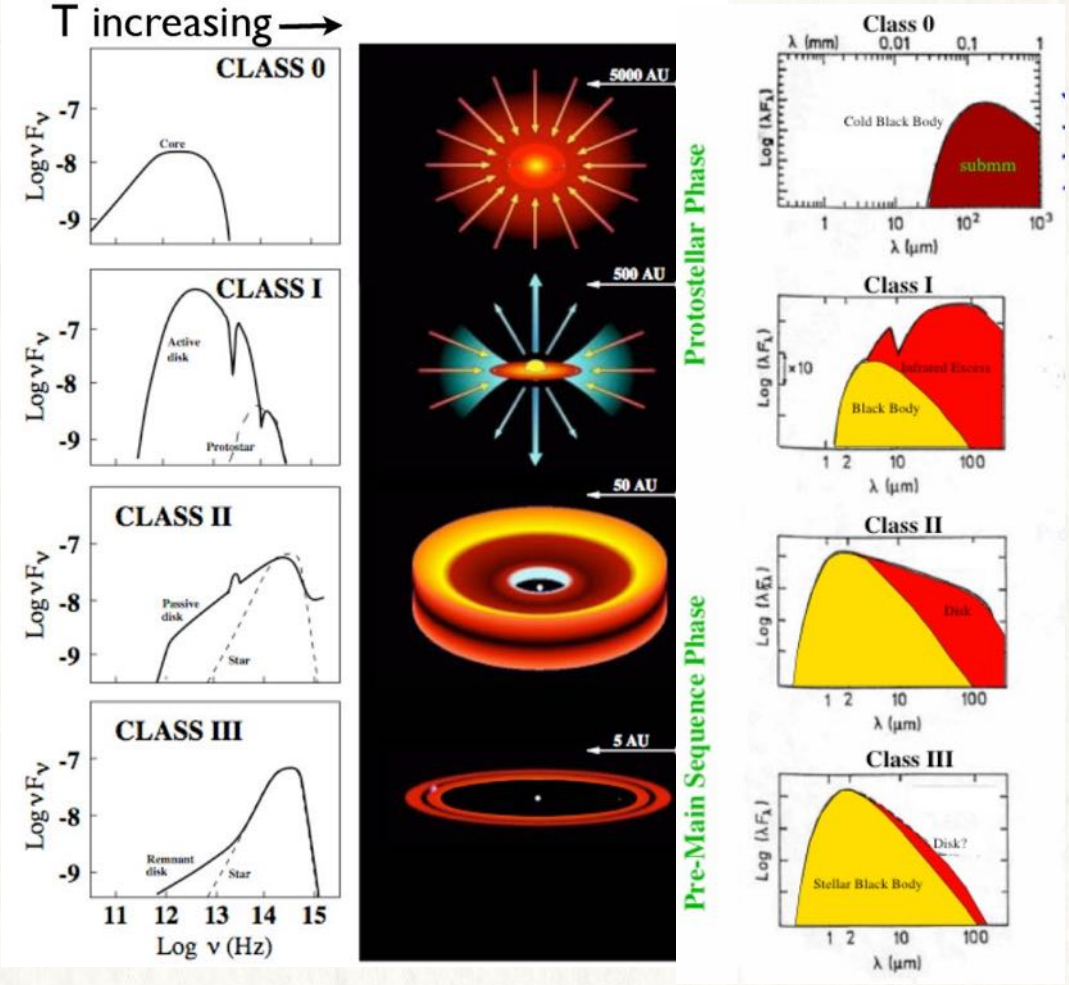

Sketch of the principal stages (Classes) of star formation (center) with the accompanying SEDs in the frequency (left) and wavelength (right) domain

The emission of the stellar photosphere is marked by the dashed line/yellow area. The contribution of the dust continuum emission (red) is diminishing over time.

(Andre+ 2002; Offner+ 2013)

A temporal increase of the accretion rate leads to an inside-out heating of the dust environment which causes a thermal afterglow. Its rise and fall will imprint on the SED.

Episodic Accretion of Low-Mass YSOs
–
From T Tauri to Proto-Stars

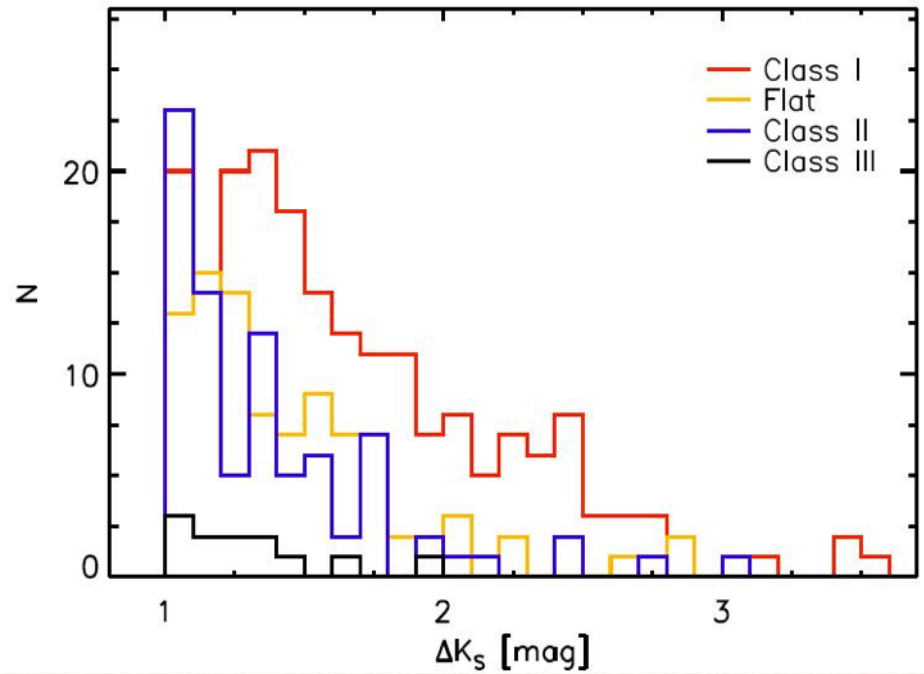

Accretion variability statistics drawn from VVV survey; confirmed by follow-up IR spectroscopy (Contreras Peña+ 2016)

More embedded objects show higher variability amplitude.

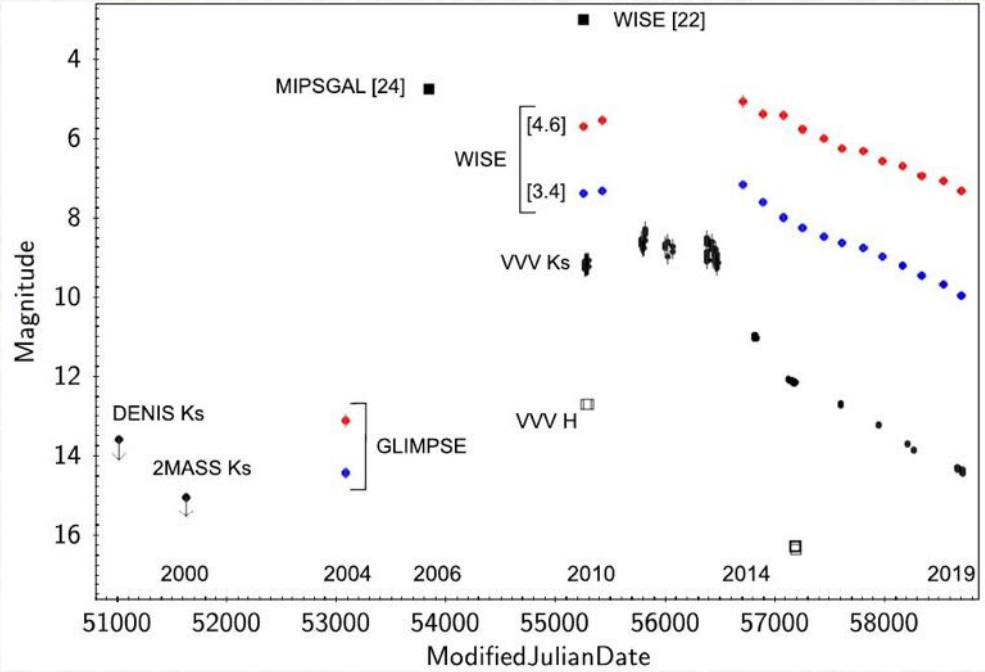

MIR protostellar outburst of WISE1422-6115, featuring an exceptional amplitude (ΔW2 ≈ 8mag, Lucas ea. 2020)

Younger objects show higher amplitudes due to their small photospheric luminosity.

Episodic Accretion of Low-Mass YSOs – From T Tauri to Proto-Stars

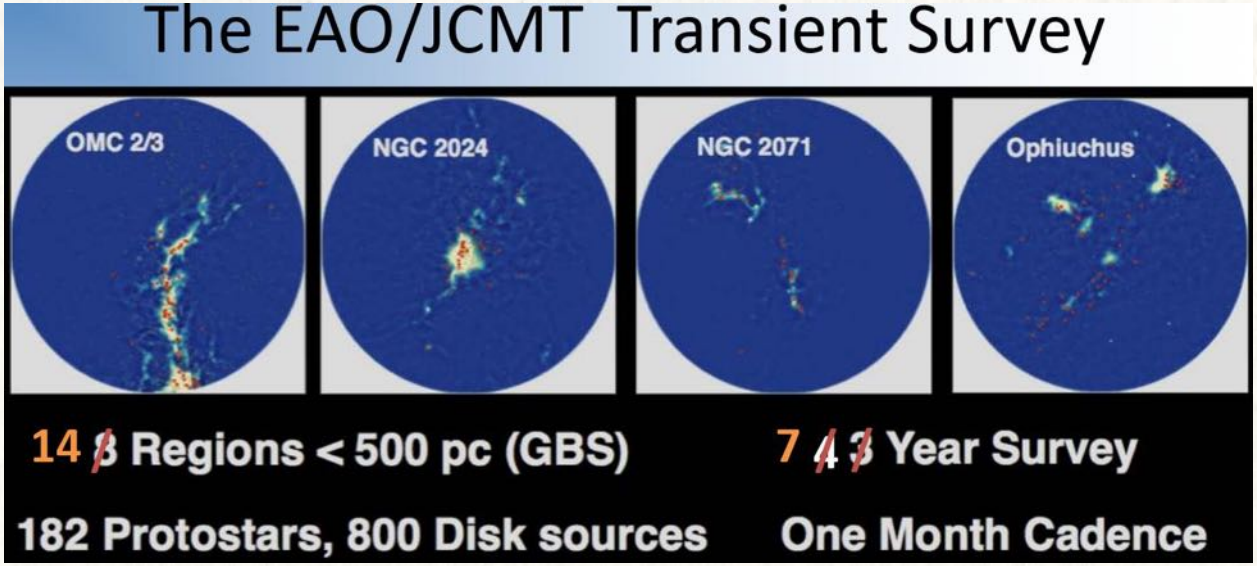

JCMT 850μm monitoring of star-forming regions (Herczeg+ 2020)

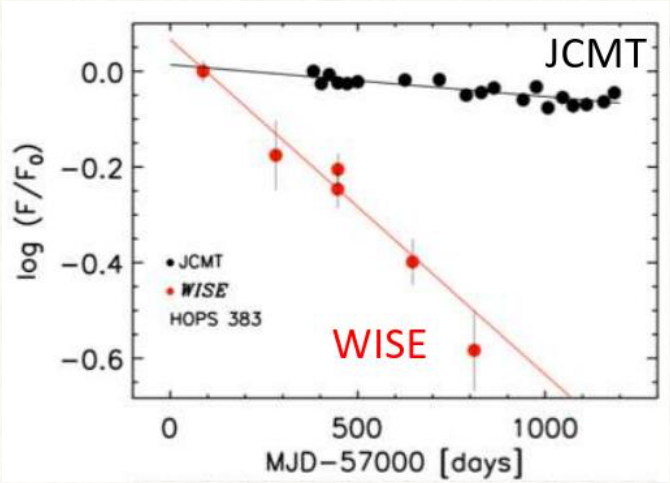

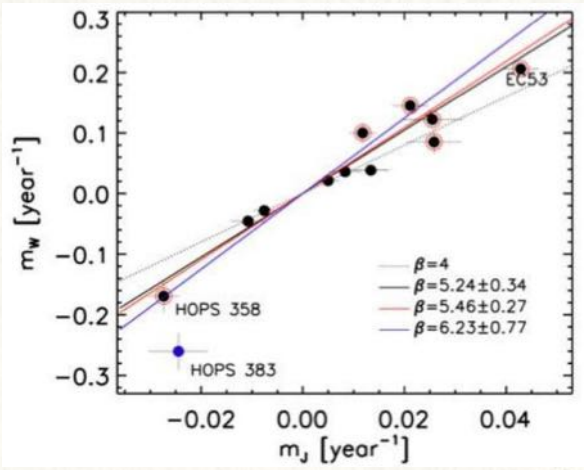

Left: The variability of submm dust continuum and MIR emission occurs on different time scales.
Right: Relation between submm and MIR time scales (Contreras Peña+ 2016)

Modeling of the Thermal Afterglow

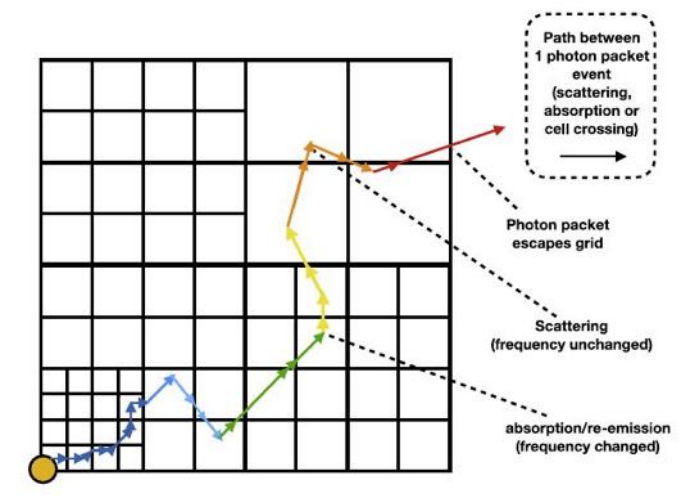

Principle of Monte Carlo radiative transfer (RT) on a grid with adaptive mesh refinement (Harries+ 2019). Color indicates wavelength.

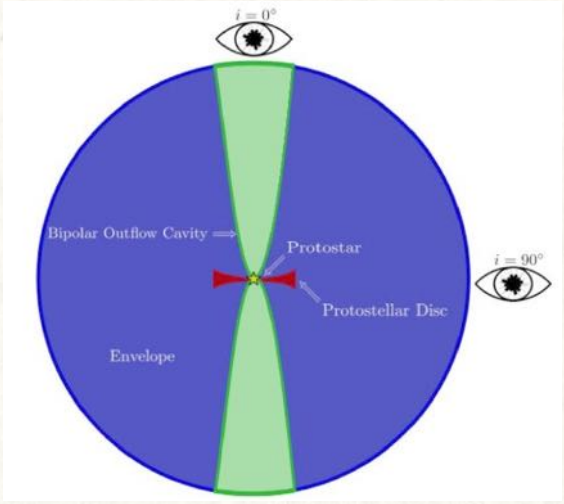

Basic YSO model and extreme viewing geometries (MacFarlane+ 2019)

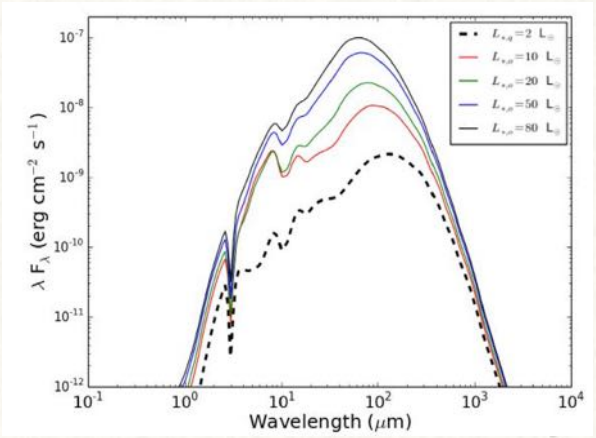

Pre-burst SED (dashed) and SEDs for various burst strengths for a low-luminosity YSO model (MacFarlane+ 2019)

$$F(\text{submm}) \propto T_{dust}$$
$$F(\text{IR}) \propto L_{acc}$$

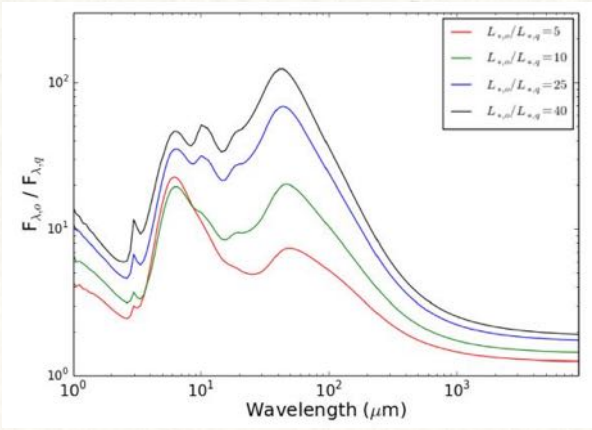

Relative flux increase for various burst strengths for a low-luminosity YSO model (MacFarlane+ 2019)

Accretion Bursts from MYSOs – An Extraordinary Coincidence

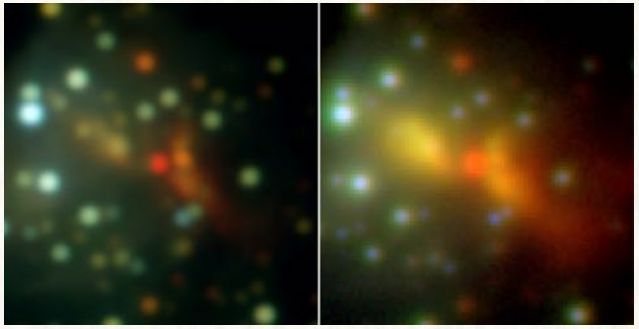

NIR pre-burst (left) and burst (right) images of S255IR-NIRS3 (Caratti o Garatti+ 2017)

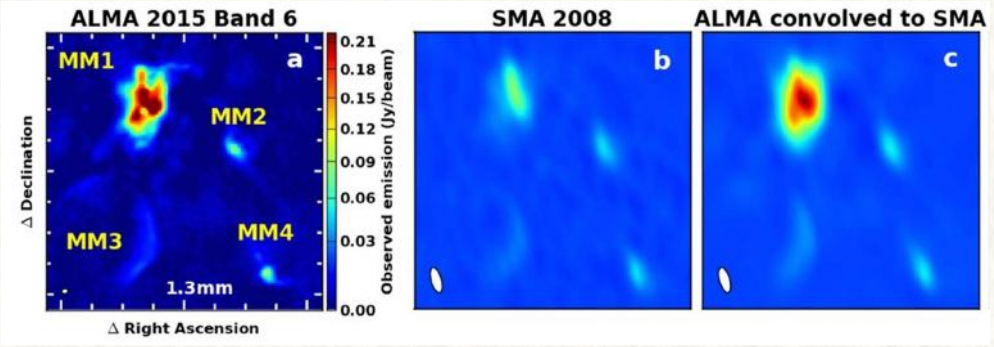

1.3mm maps of NGC6334I revealing the large emission excess from MM1 (Hunter+ 2017)

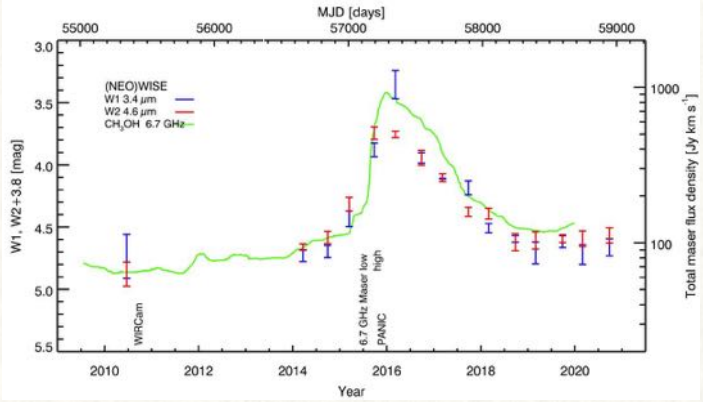

Light curves of 6.7GHz total maser flux (© M. Szymczak) und matched NEOWISE magnitudes

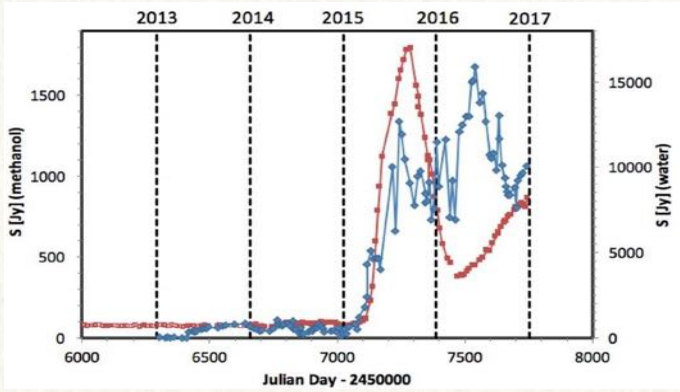

Light curves of 6.7GHz methanol (red) and 22.2GHz water (blue) total maser flux (Hunter+ 2017)

MYSOs provide sufficient specific molecular column density and MIR radiation to radiatively excite Class II methanol masers (Breen+ 2013, Cragg+ 2005)

Maser Monitoring Organization (M2O): Burst alert system based on single-dish maser monitoring, coordinated follow-up and analysis, recent MoU with JCMT

Methanol Maser Alerts – M2O's First Catch: G358

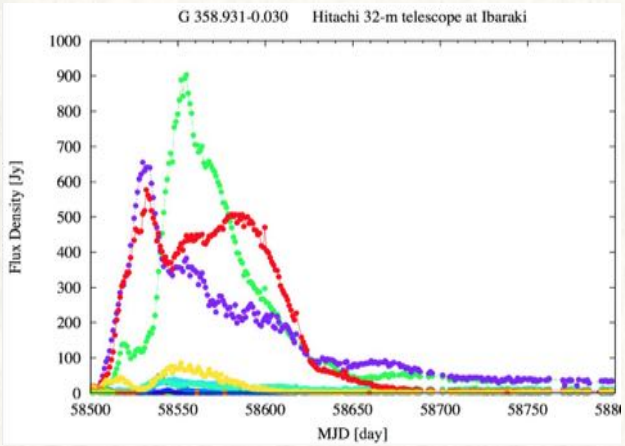

Flaring of the 6.7 GHz maser components (Sugiyama+ 2019)

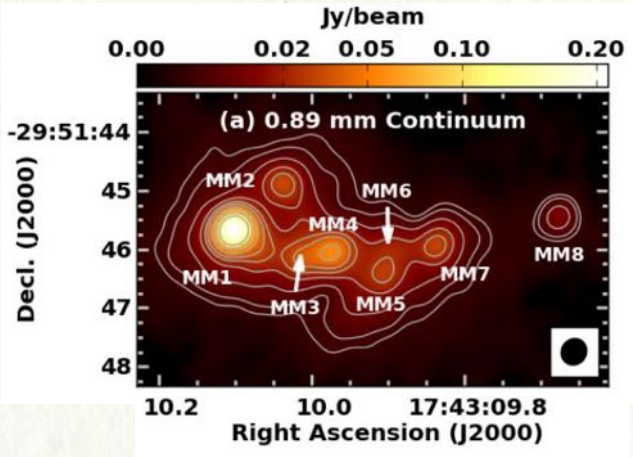

The 0.89mm ALMA map (Brogan+ 2019) reveals a proto-cluster and identifies MM1 as the maser host. No significant flux rise could be found.

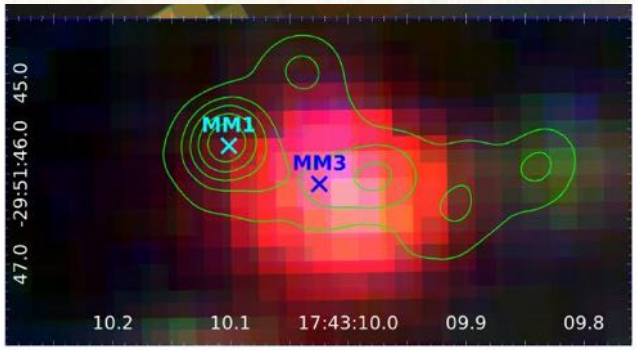

Follow-up NIR imaging with GROND does not detect MM1 (Stecklum+ 2021).

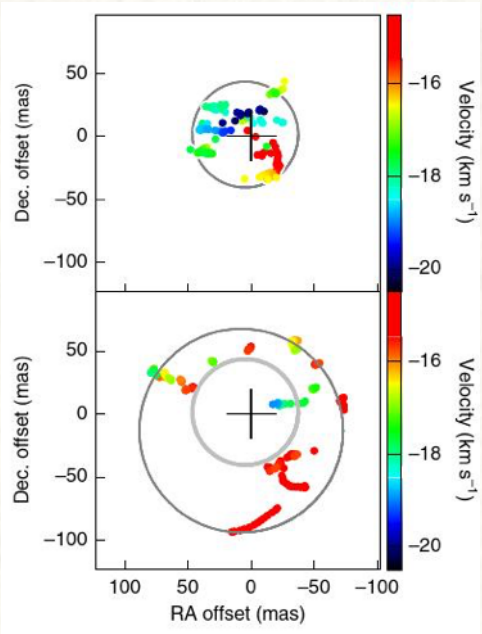

VLBI measurements reveal radial motion of maser spots at sub-luminal speed which provides evidence for the propagation of a heat wave (Burns+ 2020).

SOFIA FIFI-LS observations on 2019 May 1 (DDT) and 2020 August 28 to confirm the presence of a burst and to derive its energetics.

The FIFI-LS and archival fluxes have been used to establish and analyze SEDs for three epochs, pre-burst, burst, and post-burst.

Use of HYPERION RT code (Robitaille 2017)

Processing steps

- **SED decomposition: establish RT model for MM3, remove flux contributions of sources other than MM1 from total flux**
- **Establish pre-burst SED model for MM1 assuming inner disk radius is governed by dust sublimation**
- **Establish a pool of SEDs for various burst strengths using the pre-burst parameters for consistency**
- **Find the best models for burst- and post-burst SEDs**
- **Adopt a linear relation for the luminosity decrease over time and derive the total burst energy**

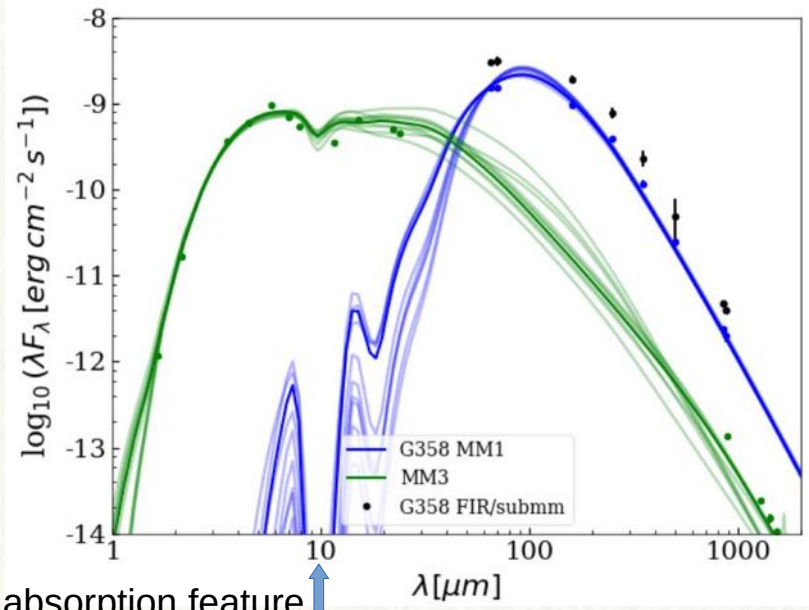

Silicate absorption feature

Fits to pre-burst SEDs of MM1 (blue) and MM3 (green). Black symbols mark total fluxes. MM1 dominates the total flux beyond 40µm.

How to “Weigh” the Accreted Mass using SOFIA

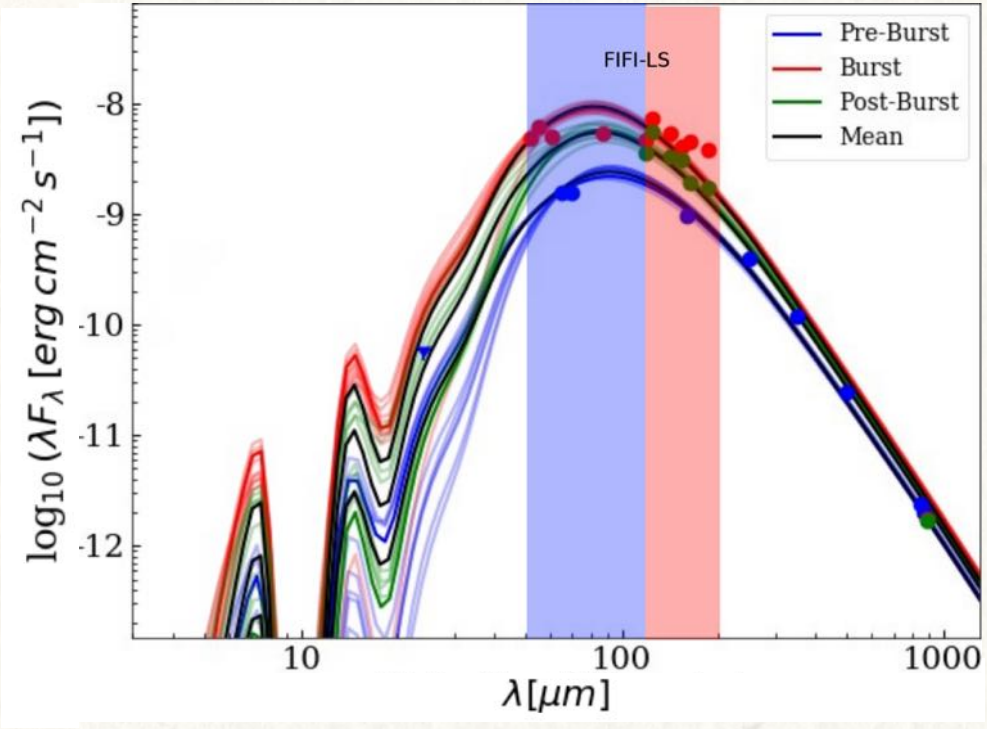

Modeled pre-burst MM1 SED (blue), together with its burst (red) and post-burst SED (green). The corresponding weighted mean-models are shown in black. Triangles mark upper limits.

Burst properties: luminosity increase $\Delta l_{acc} = (18.0\pm5.5)\times10^{3} L_\odot$

relative luminosity gain $\Delta l_{acc}/L_{pre} = 4.7\pm1.8$

total energy $E_{acc} = (2.9\pm1.0)\times10^{38}$ J

effective accretion duration $\Delta t_{acc} = 60\pm5$ days

afterglow decay time $\Delta t = 910\pm280$ days

total accreted mass $M_{acc} = (3.1\pm1.0)\times10^{-4} M_\odot$

mean accretion rate $\dot{M}_{acc} = (1.8\pm1.0)\times10^{-3} M_\odot$/yr

MM1 properties: disk mass $M_d = 3.2\times10^{-3} M_\odot$

interstellar extinction $A_V = 60\pm10$ mag

inclination $i = 22\pm11°$

stellar radius $R_* = 10.5\pm1.3 R_\odot$

stellar mass $M_* = 12\pm3 M_\odot$ (Chen+ 2020)

Heat-Wave Propagation and Maser Relocation

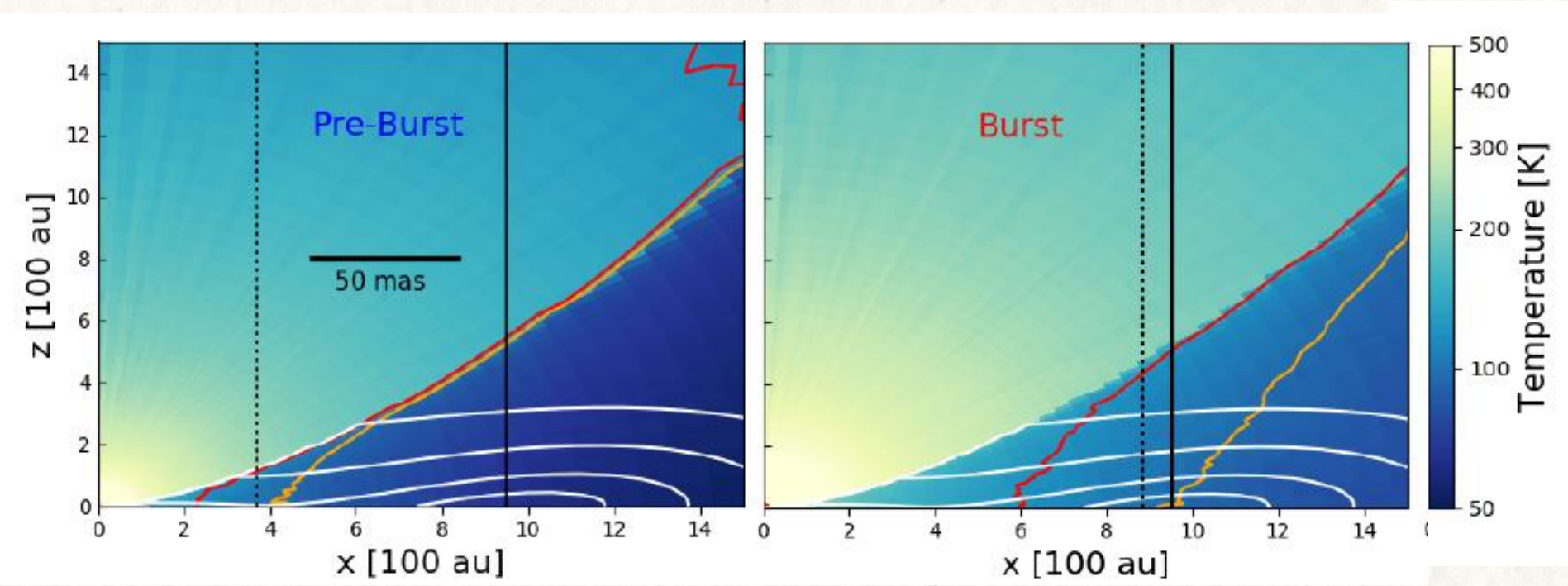

Temperature distribution of the mean model in the x-z plane (innermost part of first quadrant) for pre-burst (left) and burst (right) epochs. Orange and red lines enclose the temperature range for methanol desorption. The white contours mark gas particle volume densities which decrease with increasing z. The vertical solid black line indicates the outer radius of the disk. The dashed black lines mark the radius of the maser ring from the first and 4th epoch of the VLBI observations (Burns et al. 2020).

The static RT model seems to reproduce prime conditions for methanol maser excitation. This needs to be checked with time-dependent RT.

Implications of Accretion Bursts

Major mode for stellar mass assembly (Meyer+ 2021)

Solves the YSO under-luminosity problem (Hartmann & Kenyon 1996)

Eases the formation of massive stars by quenching UV radiation (Meyer+ 2021)

Triggering of outflow activity (Cesaroni+ 2018)

Shift of snow lines which possibly affects planet formation (Cieza 2017)

Alteration of dust grain structure due to annealing (Abraham 2009)

Change of the chemical inventory of the protostellar environment (Rab 2017)

Change of the maser landscape (Moscadelli+ 2017)

Accretion of (proto-)planets might lead to chemical enrichment of the host star (Rice+ 2006)

Accretion of (proto-)planets might lead to spin-up of the host star (Qureshi+ 2018)

Prospects – Facilities

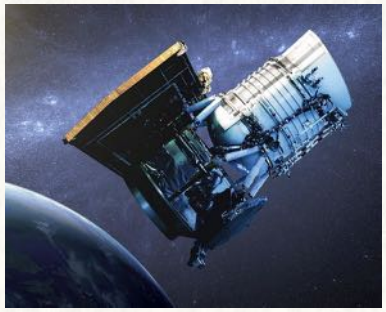
NEOWISE


ESO-VISTA


MPG-GROND


CAHA-PANIC

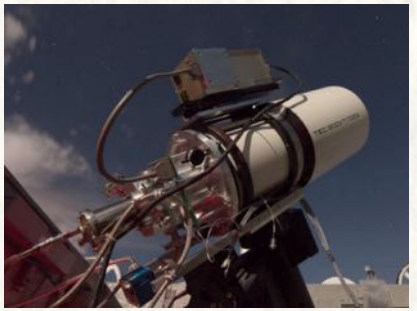
Gattini-IR

Only SOFIA provides the capability to measure the burst energy.

JWST shall reveal burst induced changes of the YSO environment.

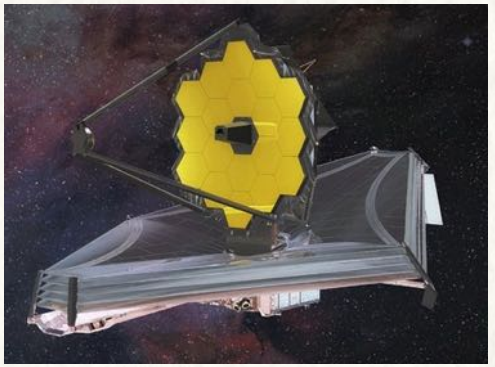

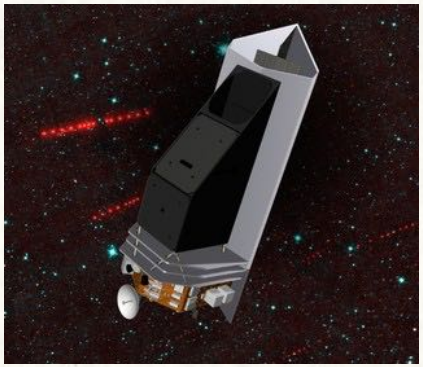

Near term IR surveys:

⟸ NEOCam (placed at L1, ecliptical survey, launch 2025)

SPHEREx ⟹ (allsky,0.5-5.0μm low-res spectroscopy, launch 2024)

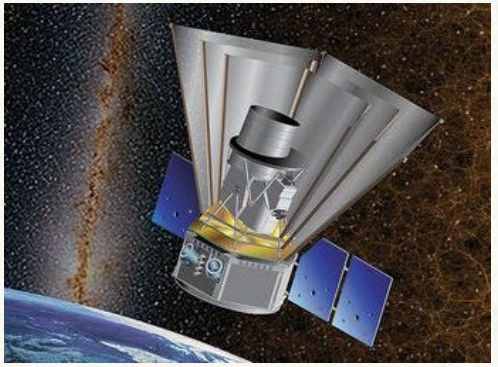

Prospects – Modeling

TORUS
The AMR radiation transport and hydrodynamics code

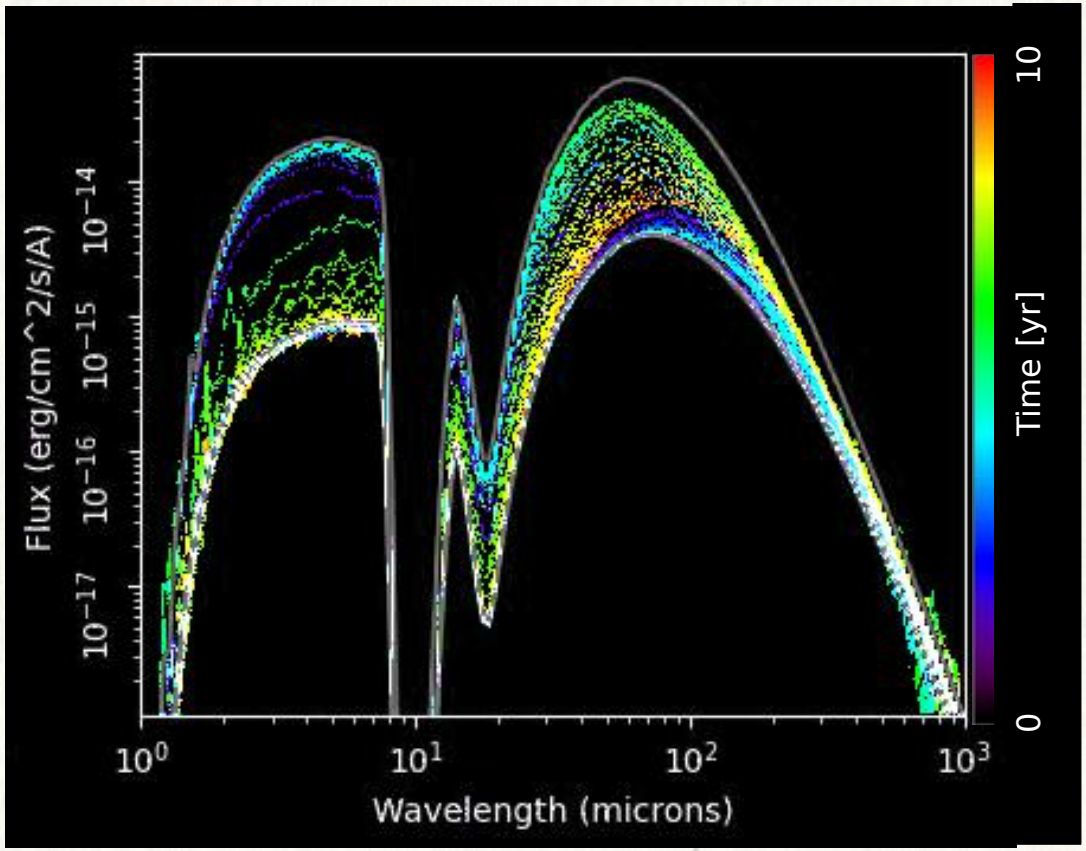

Harries (2011), Harries+ (2019)

First results of a time-dependent RT accretion burst simulation. Soon after the burst onset, NIR/MIR fluxes approach those of the static burst model while the FIR fluxes lag behind. Conversely, the NIR/MIR fluxes are almost back to the pre-burst leven when the FIR is at its maximum.

The FIR fluxes do not reach those of the static burst model since the burst was not energetic enough. Still, after 10 years they sightly exceed those of the pre-burst state.

Summary

The maser flare accompanying G358 the burst illustrates the credibility of the alert system.

The SOFIA observations confirmed the third HMYSO accretion burst.

Based on the SOFIA FIR data, our analysis yielded major burst and object properties.

Compared to the bursts of S255IR-NIRS3 and NGC6334I-MM1, that of G358 was a minor one.

Differences between the few HMYSO bursts point to a range in burst strength/duration as well as in properties and structure of the circumstellar environment.

The low disk mass found for G358 may be related to the extreme youth of this source.

Flare and afterglow time-scales must be distinguished.

The FIR excess may last for several years, allowing for an a-posteriori burst detection.